Triangularity effects on global flux-driven gyrokinetic simulations

Journal of Physics: Conference Series **2397** (2022) 012002 doi:10.1088/1742-6596/2397/1/012002

Triangularity effects on global flux-driven gyrokinetic simulations

Giovanni Di Giannatale[1], Peter Donnel[2], Laurent Villard[1], Alberto Bottino[3], Stephan Brunner[1], Emmanuel Lanti[4], Ben F. McMillan[5], Alexey Mishchenko[6], Moahan Murugappan[1], Thomas Hayward-Schneider[3]

[1] Ècole Polytechnique Féedérale de Lausanne (EPFL), Swiss Plasma Center (SPC), CH-1015 Lausanne, Switzerland
[2] CEA, IRFM, F-13108 Saint-Paul-lez-Durance, France
[3] Max-Planck-Institut für Plasmaphysik, D-85748 Garching, Germany
[4] Ècole Polytechnique Féedérale de Lausanne (EPFL), SCITAS, CH-1015 Lausanne, Switzerland
[5] CFSA, Department of Physics, University of Warwick, Coventry CV4 7AL, United Kingdom
[6] Max-Planck-Institut für Plasmaphysik, D-17491 Greifswald, Germany

E-mail: giovanni.digiannatale@epfl.ch

Abstract.
On the road to fusion energy production, many alternative scenarios have been investigated in order to address certain well-known problems of tokamak devices; among which, anomalous transport, ELMs and disruptions. The studies on plasma shaping fall into this effort.
In particular, it has been experimentally observed that when operating in L mode, negative triangularity (NT) features better confinement properties than positive triangularity (PT). However, even though the trend is quite clear, a complete and satisfying theoretical explanation for this experimental findings is still lacking.
With the aim of understanding and describing these improvements starting from first principles, we present the first comparison between PT and NT with global flux-driven gyrokinetic simulations performed with the ORB5 code.
The numerical setup includes: electrostatic turbulence, kinetic trapped electrons, non-linear collisional operator, ECRH source, limiter and wall as boundary conditions. The simulations have been performed on ideal MHD equilibria and kinetic profiles inspired by TCV experiments, in a mixed ITG-TEM regime.
First analysis reveal a strong reduction of transport in NT; while at the edge PT shows superdiffusivity, NT does not. The limiter plays an important role that has to be further clarified.

1. Introduction

Understanding and controlling the transport phenomena is notoriously one of the most challenging tasks in fusion plasmas: turbulent behavior accounts for the anomalous

transport of heat, momentum and particles in tokamak devices. Such turbulent state results from nonlinear interactions of phenomena that can develop on micro-scales and that couple to form macro-structures that affect the whole device.
Understanding the key elements of turbulence, or at least which are the parameters that affect it, would allow one to control those transport coefficients that ultimately rule the performance of a fusion device. One of the critical parameters affecting the confinement performances is the plasma triangularity δ. The TCV experiment [1] showed that in L-mode discharges with similar density profiles, the negative triangularity configurations require, with respect to positive triangularity ones, half of the electron cyclotron resonance heating (ECRH) power to sustain the same temperature profile. More recently [2] the TCV device also showed that, in ohmic discharges with similar density profiles, the fluctuations and their correlation lengths are significantly reduced when operating at $\delta < 0$. Such improvements when operating in negative triangularity have been recently observed also in the DIII-D Tokamak [3]: a NT ($\delta = -0.4$) plasma has been created with a significant normalized beta ($\beta_N = 2.7$) and confinement characteristic of the high confinement mode ($H_{98y2} = 1.2$) without featuring the dangerous feature of steep pressure gradients at the pedestal of the H-mode plasmas, that are characterized by cycles of edge localized modes (ELMs). The appealing feature of the NT is the possibility to achieve high confinement properties, similar to those observed H-mode PT plasmas, without the development of ELMs that are a crucial aspect to take into consideration when full size devices will enter in operation.
First GK simulations have shown that the plasmas where NT showed improvements with respect to PT were mostly *Trapped Electron Mode* (TEM) dominated [4]. This is consistent with the experimental evidence that the difference between PT and NT decreases when collisionality increases. It is in fact well known that collisionality has a strong effect on TEM instabilities by acting as trapping-detrapping process. In this paper, we present the first comparison between PT and NT with global flux-driven gyrokinetic simulations in a mixed ITG-TEM regime. The analysed configurations, inspired from TCV shots, are highly shaped ($\delta \sim \pm 0.5$) and a significant difference between the two scenarios has been numerically observed.

2. Numerical setup

The gyrokinetic simulations presented in this work have been performed with the ORB5 code [5]. ORB5 is a global gyrokinetic code using a PIC approach and finite element representation. In spite of the δf splitting which is used as control variate, it is a "full-f" code. The only ordering assumption is in the polarization term, linearized around the initial distribution function. The gyrokinetic Vlasov–Maxwell model implemented in ORB5 is derived from a variational principle [6, 7] which makes completely consistent all the subsequent approximations made in the model.
The code uses a magnetic straight-field-line coordinate system (s, θ_*, ϕ), with $s = \sqrt{(\psi/\psi_a)}$ (ψ poloidal flux), θ_* poloidal angle-like coordinate and ϕ toroidal angle. The quasineutrality and Ampère equations are based on a 3D finite elements representation considering linear, quadratic, or cubic B-splines. Then, the resulting linear system is projected into Fourier space in order to decouple the various harmonics and to save computational time by retaining only the modes of interest [8, 5]. The code can handle

efficiently electromagnetic perturbations [9], though this paper focuses on electrostatic runs.
Besides the continuous computational improvements, recently the code has been through few physics modeling improvements such as the renewal of the collisionality operator [10] and the implementation of the ECRH source [11] that allows realistic flux driven simulations.

The simulations have been performed on ideal MHD equilibria and kinetic profiles inspired by TCV experiments. The magnetic configuration has been obtained with the CHEASE code [12]. The equilibria are inspired by the shots #60797 ($\delta > 0$) and #58499 ($\delta < 0$). The equilibria are consistent with TCV data until the last closed flux surface (LCFS), then in order to include the boundary region in ORB5 (see later) a flat pressure profile is inserted. Such an ad-hoc region is meaningless from a physical point of view and we do not discuss that region; the results will be analyzed up to slightly after the LCFS, where the triangularity values are $\delta \sim \pm 0.5$.

To give an idea of how much the system evolves, the initial electron temperature profile is shown together with the temperature at an advanced stage of the simulation in figure 1. The initial temperature in the boundary region ($\rho_{vol} \in [0.9, 1]$) is flat.

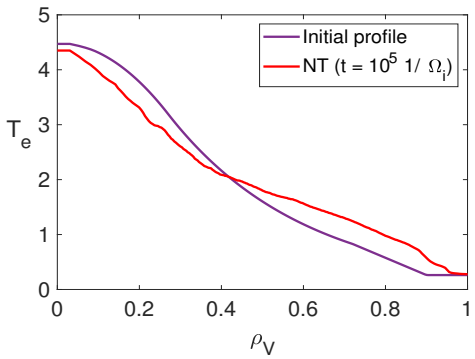

Figure 1: Initial electron temperature profile (purple) used to start the GK simulations and temperature after 10^5 $1/\Omega_i$ (NT case).

The boundary region is modeled to simulate the scrape of layer (SOL) with the last closed flux surface (LCFS) located at $\rho_{vol} = 0.9$, with $\rho_{vol} = \sqrt{(V(\psi)/V(\psi_a))}$. In order to take into account part of the SOL effects, ORB5 adopts the same limiter modeling introduced in GYSELA [13]. To do so, we apply a penalization term to the distribution function acting in the limiter. In this region (poloidally localized between $\theta_* \in [3/2\pi - \Delta, 3/2\pi + \Delta]$), the distribution function is damped according to:

$$\frac{\partial \delta f}{\partial t} = -\gamma(s)\, \delta f \ , \tag{1}$$

where $s = \sqrt{\hat{\psi}}$ ($\hat{\psi}$ normalized poloidal flux) and $\gamma(s) = \gamma_0/2 + \gamma_0/2 \tanh(\alpha(s - s_{LCFS}))$, with γ_0 damping coefficient and α "transition" coefficient. In addition to the limiter, also the "wall" has been inserted.

The wall is a radially narrow and polodailly symmetric damping region surrounding the whole plasma volume ($\rho_{vol} \in [0.98, 1]$). Finally, also the Quasi-neutrality equation (QNE) is slightly modified (see [13]). The QNE now reads

$$-\mathcal{P}[\phi] + \alpha n_{e0} \frac{n_{e0}}{T_e}(\phi - (1 - M^{SOL})\langle\phi\rangle) = \rho. \tag{2}$$

The first term, $\mathcal{P}[\phi]$, is the Polarization term (it is left in its generical functional form since its shape can depend on the approximations done, see [14]), the second term corresponds to the adiabatic response of the passing electrons (α is the passing fraction) and finally ρ is the gyrocenter charge density (in this term the contribution of electrons comes from trapped ones only). M^{SOL} is a geometrical mask : it is null before the LCFS and one beyond it. The term $1 - M^{SOL}$ is inserted because after the LCFS closed field lines do not exist anymore and it is thus meaningless to remove the averaged potential. Further details about the limiter will be presented in a future paper together with a detailed study on the effects of such modeling.

The multispecies collisional operator [10] is used and the flux driven simulation is sustained by the ECRH source [11] that operates with a power of 200kW.

The noise, inevitable drawback of PIC simulations [15, 16], deserves special care. Features as collisions and ECRH heating increase drastically the noise since such operators are applied in form of Langevin equations, solved with random kicks in phase space. For such reason, it is prohibitive to carry out a unique long simulation. For this kind of simulations also the polarization density, that is the only *not* full-f feature of the code, deserves special attention. Usually such assumption is not dramatically important, but when the limiter is taken into account the edge plasma experience a substantial density deviation with respect to its initial state.
To partially solve the noise problem and take into account the evolution of polarization density, after a substantial simulation time, the density and the temperature are collected and used as new profiles for another simulation. This process is repeated few times. These profiles are obtained averaging over a time window such that we can average out all the fast fluctuations, included avalanches. Usually this time window corresponds to $5\ 10^3\ [\Omega_i^{-1}]$.

Unfortunately starting a new simulation is time demanding since the system has to go through the turbulence develop. For this reason, when the noise is low enough, the update of the initial distribution function is done during the simulation, without restarting a new one. To do this, one has to change the weights of the markers. Under the PIC approach, δf is represented by markers as follows:

$$\delta f = \sum_{p=1}^{N_p} \frac{w_p(t)}{J(\mathbf{Z})} \delta(\mathbf{Z} - \mathbf{Z}_p) \tag{3}$$

where $\mathbf{Z}$ is a set of generalized phase-space coordinates, $\mathbf{Z}_p$ is the orbit of the p-th marker in phase space, $J(\mathbf{Z})$ is the Jacobian associated with the coordinates $\mathbf{Z}$ and w_p is the weight of the p-th marker. Inserting part of δf inside f_0 requires moving part of the δf weight inside the f_0 weight. For each marker both a δf and a f_0 weight are needed when collisions are taken into account, and the change in f_0 translates in the change

of its weight. We do this procedure not continuously but only at discrete times. It is important at this point to also recompute, considering the new f_0, all the terms that we need to solve the QNE. It is important to remark that the total weight, representing the whole distribution function, cannot be changed by this procedure: it is indeed a good check to verify that temperature and density are not changed in this "adaptation".

Without adapting the distribution function, the linearized polarization density prevents the density to evolve as it would if the non-linear behavior was taken into account. This is shown in figure 2. Here during a simulation we applied the adaptation two times as we can see from the jumps of the density.
A proper continuous adaptation scheme has been lately inserted in ORB5. Such a scheme will enable nonlinear evolution of polarization density but also a huge reduction of the noise as it is shown in [17].

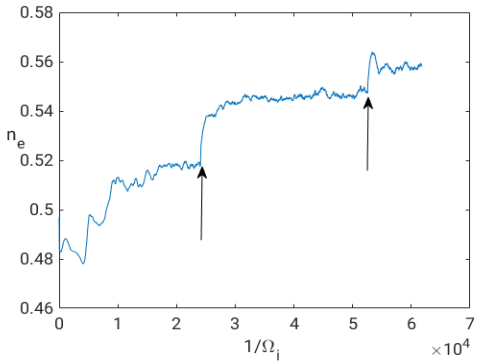

Figure 2: Time evolution of the electron density at $s = 0.95$. The arrows mark the temporal instant where the adaptation of the f_0 is done.

3. Simulation results

The simulations have been performed with 800 millions of markers for each species (deuterium and electrons). The grid for the quasi-neutrality equation is $N_s \times N_{\theta_*} \times N_\phi = 256 \times 512 \times 256$. A field-aligned Fourier filter is applied with $\Delta m = 5$; with (m, n) the poloidal and toroidal mode numbers, respectively. The filter assures that only certain m, that is $m \in [nq - \Delta m,\ nq + \Delta m]$, are considered. Moreover, due to the grid resolution is not possible to reach arbitrary wavenumbers, thus, on top of the filter, we consider only $n \in [0, 32]$ and $m \in [-64, 64]$. The time step is set to 1, in units normalized to the ion cyclotron frequency. The initial distribution function is a local Maxwellian. It turns out that the turbulence is the result of an ITG-TEM mixed regime.

3.1. Zonal Flows and avalanches

It is well known that the transport properties and the turbulence effects are strongly related to the structure of the zonal flow and its shearing rate. The zonal flow (ZF), see [18] for a complete review, is a toroidally symmetric electric field perturbation in a toroidal plasma, which is constant on the magnetic surface but rapidly varies in the

radial direction. It is the result of a non-linear interaction, which transfer energy from the finite-n drift waves to the $n = 0$ flow. Once it is developed, the ZF strongly acts on turbulence itself giving rise to a self-organization process. Strong radial shears of ZFs are helpful for transport reduction: they stretch and tear apart turbulence vortexes.

The ZF shearing rates are shown, together with the electrons heat fluxes, in figure 3. In the core there is not a qualitative difference between the two cases, whereas at the edge a difference shows up. Both configurations exhibit avalanches also in the shearing rate but for PT they are very clear and easy to recognize: there is a coherent behaviour. This is not the case for the NT configuration where a more tangled behaviour can be observed. The PT case has a well define frequency whereas the NT case does not.
In both cases the avalanches are triggered at the edge and the boundary condition, i.e. the limiter, plays a crucial role that will be investigated in a forthcoming paper.
From the color map can be seen that a strong shearing rate rises at the edge, where there is the LCFS. From a first analysis, the spikes can be partially due to the limiter [13]. The QNE experiences a "*modelling* discontinuity" when going through the LCFS: the density is damped and the averaged potential is not substracted anymore in the adiabatic response. This means that the left hand side of Eq 2 has a positive increment and the right hand side has a negative one (the density damping only happens in the limiter and close to the wall).

3.2. Transport mechanism

As we showed, both configurations feature heat flux avalanches (the same behaviour is found also for the particle flux).

As is well known, the plasma does not always feature local transport [19] especially when the system exhibits avalanches [20]. We try somehow to characterize how far from diffusive is our plasma transport. As a first attempt we compute the Hurst exponent H [21] using both the method of the autocorrelation [22] and the RS method [23]. Such exponent can be related to the kind of transport: diffusive ($H = 0.5$), sub-diffusive($H < 0.5$), super-diffusive($H > 0.5$). In few words, an Hurst exponent bigger than 0.5 means that the subsequent increments of the signals are positively correlated while with $H < 0.5$ the subsequent increments would be anti-correlated.
Computing a reliable coefficient is not an easy task since it may be sensitive to several parameters, such as noise in the data, sampling size, time windows and subsets considered to build the power law. Thus, using both methods, we varied few numerical parameters (used to compute the Hurst exponent) and we evaluate the average among the several H-exponents. For both configurations we took a time window of $3\,10^4[\Omega_i^{-1}]$ and within this window we carried out the Hurst computations. We moved such time window in order to be less sensitive to the window under examination. We varied also the batch sizes for the RS method.

The resulting radial profiles of the Hurst exponent for the electron temperature is shown in figure 4, together with the error bars.

It is quite clear that there is an important difference between core and edge. Around $s = 0.7$ there is not any remarkable difference between positive and negative triangularity; the process is diffusive ($H = 0.5$). As we move towards the edge, a difference between

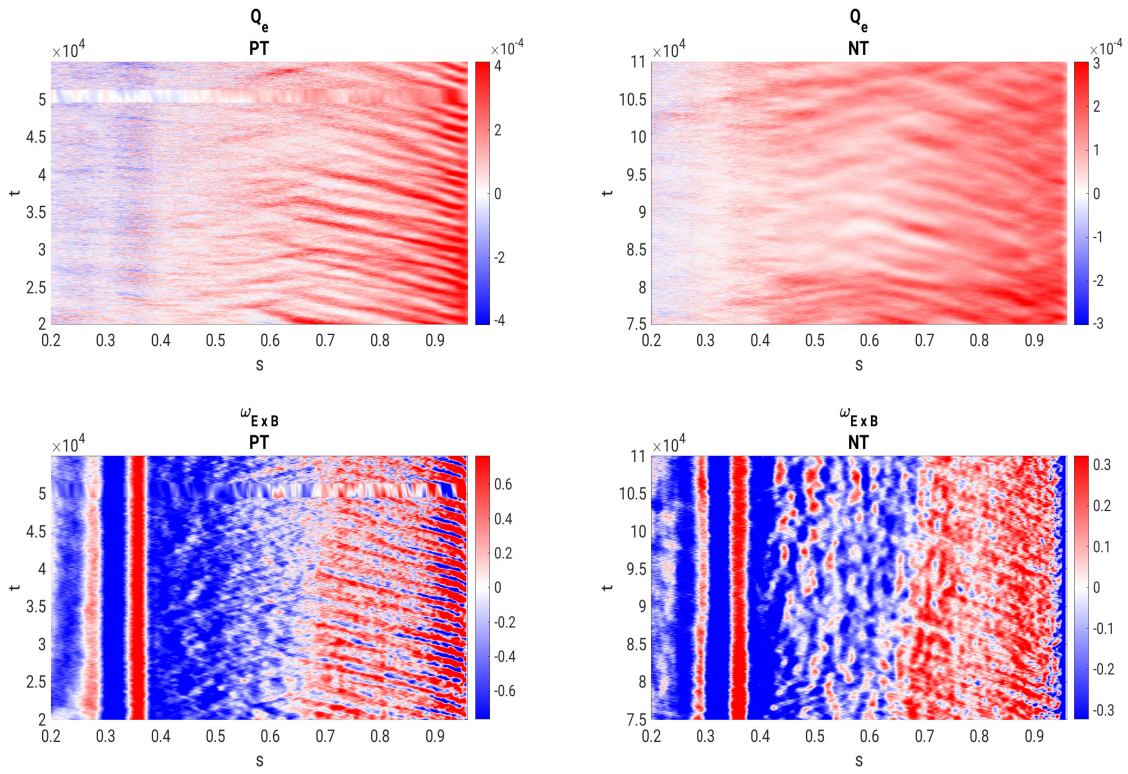

Figure 3: 2D (radial coordinate - time) plot of the electron heat flux (top raw) and shearing rate (bottom raw) in positive and negative triangularity configuration, left and right panel respectively. To not spoil the colorbar with outliers, they are normalized to the max value inside the 90^{th} percentile.

positive and negative triangularity shows up. According to the error bars, the result is very robust for electrons. This result confirms once again that the transport is not always local and cannot be always approximated as so.
We note that for positive triangularity the super-diffusive transport ($H > 0.5$) penetrates radially much more than for NT. Thus we can tentatively attribute the lower PT confinement time to enhanced nonlocal transport from the edge to the core.

4. Conclusions

In this preliminary paper we presented the first comparison between positive and negative triangularity with global flux-driven gyrokinetic simulations performed with the ORB5 code. The numerical setup includes the limiter feature that seems to trigger avalanches and non-local transport. The heat flux and the shearing rate appear different for the two configurations, requiring further in-depth studies. A more quantitative approach such as the Hurst exponent underlines that positive triangularity has a stronger non locality and

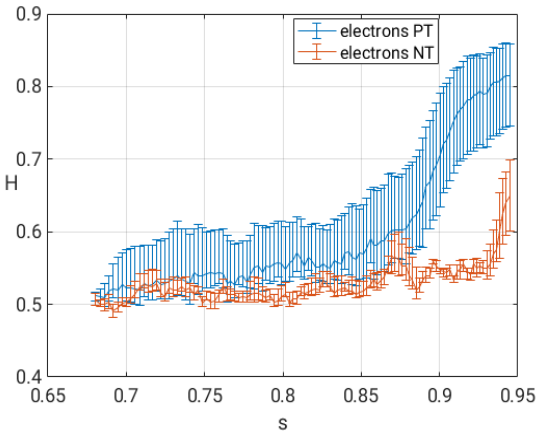

Figure 4: Hurst exponent profile (with error bars) for electron temperature for positive and negative triangularity, blue and red respectively.

superdiffusive behaviour. We can tentatively speculate that this is consistent with the fact that PT has a lower confinement time with respect to the NT that in turns exhibits a lower Hurst coefficient.

In forthcoming papers the authors will present results on the confinement time, showing that GK simulations confirm the same trend of the experiments, and a detailed study on the effects of the limiter.

References

[1] Y. Camenen, A. Pochelon, R. Behn, A. Bottino, A. Bortolon, S. Coda, A. Karpushov, O. Sauter, G. Zhuang, and the TCV team, "Impact of plasma triangularity and collisionality on electron heat transport in TCV l-mode plasmas," *Nuclear Fusion*, vol. 47, pp. 510–516, jun 2007.

[2] M. Fontana, L. Porte, S. Coda, O. Sauter, and T. T. Team, "The effect of triangularity on fluctuations in a tokamak plasma," *Nuclear Fusion*, vol. 58, p. 024002, dec 2017.

[3] M. E. Austin, A. Marinoni, M. L. Walker, M. W. Brookman, J. S. deGrassie, A. W. Hyatt, G. R. McKee, C. C. Petty, T. L. Rhodes, S. P. Smith, C. Sung, K. E. Thome, and A. D. Turnbull, "Achievement of reactor-relevant performance in negative triangularity shape in the diii-d tokamak," *Phys. Rev. Lett.*, vol. 122, p. 115001, Mar 2019.

[4] G. Merlo, S. Brunner, O. Sauter, Y. Camenen, T. Görler, F. Jenko, A. Marinoni, D. Told, and L. Villard, "Investigating profile stiffness and critical gradients in shaped TCV discharges using local gyrokinetic simulations of turbulent transport," *Plasma Physics and Controlled Fusion*, vol. 57, p. 054010, apr 2015.

[5] E. Lanti, N. Ohana, N. Tronko, T. Hayward-Schneider, A. Bottino, B. McMillan, A. Mishchenko, A. Scheinberg, A. Biancalani, P. Angelino, S. Brunner, J. Dominski, P. Donnel, C. Gheller, R. Hatzky, A. Jocksch, S. Jolliet, Z. Lu, J. Martin Collar, I. Novikau, E. Sonnendrücker, T. Vernay, and L. Villard, "Orb5: A global electromagnetic gyrokinetic code using the pic approach in toroidal geometry," *Computer Physics Communications*, vol. 251, p. 107072, 2020.

[6] H. Sugama, "Gyrokinetic field theory," *Physics of Plasmas*, vol. 7, no. 2, pp. 466–480, 2000.

[7] N. Tronko, A. Bottino, and E. Sonnendrücker, "Second order gyrokinetic theory for particle-in-cell

codes," *Physics of Plasmas*, vol. 23, no. 8, p. 082505, 2016.

[8] B. McMillan, S. Jolliet, A. Bottino, P. Angelino, T. Tran, and L. Villard, "Rapid fourier space solution of linear partial integro-differential equations in toroidal magnetic confinement geometries," *Computer Physics Communications*, vol. 181, no. 4, pp. 715–719, 2010.

[9] A. Mishchenko, A. Bottino, A. Biancalani, R. Hatzky, T. Hayward-Schneider, N. Ohana, E. Lanti, S. Brunner, L. Villard, M. Borchardt, R. Kleiber, and A. Könies, "Pullback scheme implementation in orb5," *Computer Physics Communications*, vol. 238, pp. 194–202, 2019.

[10] P. Donnel, X. Garbet, Y. Sarazin, V. Grandgirard, Y. Asahi, N. Bouzat, E. Caschera, G. Dif-Pradalier, C. Ehrlacher, P. Ghendrih, C. Gillot, G. Latu, and C. Passeron, "A multi-species collisional operator for full-f global gyrokinetics codes: Numerical aspects and verification with the gysela code," *Computer Physics Communications*, vol. 234, pp. 1–13, 2019.

[11] P. Donnel, J. Cazabonne, L. Villard, S. Brunner, S. Coda, J. Decker, M. Murugappan, and M. Sadr, "Quasilinear treatment of wave–particle interactions in the electron cyclotron range and its implementation in a gyrokinetic code," *Plasma Physics and Controlled Fusion*, vol. 63, p. 064001, apr 2021.

[12] H. Lütjens, A. Bondeson, and O. Sauter, "The chease code for toroidal mhd equilibria," *Computer Physics Communications*, vol. 97, no. 3, pp. 219–260, 1996.

[13] E. Caschera, *Global confinement properties of Tokamak plasmas in global, flux-driven, gyrokinetic simulations*. PhD thesis, Aix-Marseille Université, Marseille, France, 2019.

[14] E. Lanti, N. Ohana, N. Tronko, T. Hayward-Schneider, A. Bottino, B. McMillan, A. Mishchenko, A. Scheinberg, A. Biancalani, P. Angelino, S. Brunner, J. Dominski, P. Donnel, C. Gheller, R. Hatzky, A. Jocksch, S. Jolliet, Z. Lu, J. Martin Collar, I. Novikau, E. Sonnendrücker, T. Vernay, and L. Villard, "Orb5: A global electromagnetic gyrokinetic code using the pic approach in toroidal geometry," *Computer Physics Communications*, vol. 251, p. 107072, 2020.

[15] A. Y. Aydemir, "A unified monte carlo interpretation of particle simulations and applications to non-neutral plasmas," *Physics of Plasmas*, vol. 1, no. 4, pp. 822–831, 1994.

[16] S. E. Parker and W. W. Lee, "A fully nonlinear characteristic method for gyrokinetic simulation," *Physics of Fluids B: Plasma Physics*, vol. 5, no. 1, pp. 77–86, 1993.

[17] M. Murugappan, L. Villard, S. Brunner, B. F. McMillan, and A. Bottino, "Gyrokinetic simulations of turbulence and zonal flows driven by steep profile gradients using a delta-f approach with an evolving background maxwellian," 2022.

[18] P. H. Diamond, S.-I. Itoh, K. Itoh, and T. S. Hahm, "Zonal flows in plasma—a review," *Plasma Physics and Controlled Fusion*, vol. 47, pp. R35–R161, apr 2005.

[19] G. Dif-Pradalier, P. H. Diamond, V. Grandgirard, Y. Sarazin, J. Abiteboul, X. Garbet, P. Ghendrih, A. Strugarek, S. Ku, and C. S. Chang, "On the validity of the local diffusive paradigm in turbulent plasma transport," *Phys. Rev. E*, vol. 82, p. 025401, Aug 2010.

[20] L. Villard, B. F. McMillan, E. Lanti, N. Ohana, A. Bottino, A. Biancalani, I. Novikau, S. Brunner, O. Sauter, N. Tronko, and A. Mishchenko, "Global turbulence features across marginality and non-local pedestal-core interactions," *Plasma Physics and Controlled Fusion*, vol. 61, p. 034003, feb 2019.

[21] H.R.Hurst, "Long-term storage in reservoirs," *Trans. Amer. Soc. Civil Eng*, vol. 116, pp. 770–799, 1951.

[22] T. D. Matteo, "Multi-scaling in finance," *Quantitative Finance*, vol. 7, no. 1, pp. 21–36, 2007.

[23] J. Mielniczuk and P. Wojdyłło, "Estimation of hurst exponent revisited," *Computational Statistics Data Analysis*, vol. 51, no. 9, pp. 4510–4525, 2007.